Atti Accademia Nazionale dei Lincei

Classe Scienze Fisiche Matematiche Naturali

Rendiconti

Giacinto Porco, Giuseppe Spadea, Raffaele Zinno

A geometrically nonlinear analysis of laminated composite plates using a shear deformation theory

Atti della Accademia Nazionale dei Lincei. Classe di Scienze Fisiche, Matematiche e Naturali. Rendiconti, Serie 8, Vol. **83** (1989), n.1, p. 159–176.

Accademia Nazionale dei Lincei

<http://www.bdim.eu/item?id=RLINA_1989_8_83_1_159_0>

Atti della Accademia Nazionale dei Lincei. Classe di Scienze Fisiche, Matematiche e Naturali. Rendiconti, Accademia Nazionale dei Lincei, 1989.

Atti Acc. Lincei Rend. fis.
(8), LXXXIII (1989), pp. 159-176

Meccanica. — *A geometrically nonlinear analysis of laminated composite plates using a shear deformation theory.* Nota di GIACINTO PORCO (*), GIUSEPPE SPADEA (*) e RAFFAELE ZINNO (*), presentata (**) dal Socio E. GIANGRECO.

ABSTRACT. — A shear deformation theory is developed to analyse the geometrically nonlinear behaviour of layered composite plates under transverse loads.

The theory accounts for the transverse shear (as in the Reissner Mindlin plate theory) and large rotations (in the sense of the von Karman theory) suitable for simulating the behaviour of moderately thick plates.

Square and rectangular plates are considered: the numerical results are obtained by a finite element computational procedure and are given for various boundary and loading conditions, a/b ratios, stacking and orientation of layers and material properties (E_1/E_2 ratio, E_1/G ratio, etc.).

KEY WORDS: Plates; Composite; Laminated.

RIASSUNTO. — *Sul comportamento non lineare di piastre laminate composite.* In questo lavoro si sviluppa una teoria che tiene conto della deformabilità tagliante allo scopo di analizzare il comportamento di piastre laminate composite sottoposte a carichi flettenti.

La teoria tiene conto delle deformazioni dovute al taglio (nel senso della teoria delle piastre spesse di Reissner-Mindlin) e di rotazioni moderatamente grandi (nel senso della teoria di von Karman).

I risultati numerici, relativi a piastre rettangolari, sono stati ottenuti attraverso una procedura computazionale agli elementi finiti considerando varie condizioni di vincolo e di carico, diversi valori del rapporto a/b, differenti spessori ed orientazioni delle lamine e proprietà dei materiali (rapporto E_1/E_2, rapporto E_1/G, etc.).

NOTATION

A_{ij}, B_{ij}, D_{ij}	Extensional, flexural-extensional and flexural stiffness ($i, j = 1, 2, 3$)
H_{ij}	Thickness shear stiffness ($i, j = 4, 5$)
a, b	Plate dimensions along the X and Y directions, respectively
E_1, E_2	Layer elastic moduli in directions along fibres and normal to them, respectively
G_{12}, G_{13}, G_{23}	Layer in-plane and thickness shear moduli
h	Total thickness of the laminate
t_k	Thickness of k-th layer
K	Shear correction coefficient
x, y, z	Position coordinates in a cartesian system
M_i, N_i	Stress couples and stress resultants, respectively ($i = x, y, xy$)
Q_i	Shear stress resultants ($i = x, y$)
u, v, w	Displacements in the x, y, z directions, respectively
u_0, v_0, w_0	Displacements of the midplane in the x, y, z directions, respectively
θ^k	Orientation of the k-th layer
ψ_x, ψ_y	Slopes in the xz and yz planes
χ_x, χ_y, χ_{xy}	Curvature components
ε_x, ε_y, ε_{xy}	Strain components
ε_x^0, ε_y^0, ε_{xy}^0	Middle surface strain components
n	Number of layers
q_0	Uniform transverse load
N	Number of global nodes of the mesh in the F.E.M. discretization

(*) Dipartimento di Strutture, Università della Calabria - 87030 Arcavacata di Rende (Cs), Italy.
(**) Nella seduta del 13 maggio 1989.

ν_{ij}	Poisson's ratios ($i, j = 1, 2$ $(i \neq j)$)
$\overline{C}_{ij}^{k}$	Material stiffness coefficient (local system) of the k-th layer
C_{ij}^{k}	Material stiffness coefficient (global system) of the k-th layer
T^{k}	Transformation matrix of the k-th layer
f_i	Interpolation functions

Introduction.

In the last two decades laminated plates have become an important structural element widely applied in the aerospace, medical, automotive and electronics industries [16].

This is mainly due to their high stiffness-to-weight ratio, coupled with the flexibility in the selection of the laminate scheme that can be tailored to match the design requirements. A comparison of results obtained from the classical plate theory (CPT) with the exact elasticity solutions indicates the necessity of considering transverse shear deformation in the analysis of layered composite plates [4].

In fact transverse shear effects are more pronounced in composite laminated plates than in isotropic plates because of their low transverse shear moduli relative to the in-plane Young's moduli ($25 \div 40$ instead of 2.6, typical of isotropic materials).

Unfortunately, much of the previous research in this field is limited to linear problems and the main results are based on the classical thin-plate theory, which neglects transverse shear deformation effects [3].

The work associated with anisotropic plates with an arbitrary number of layers reached a peak in 1969.

Whitney and Leissa [17] formulated the governing equations of generally laminated anisotropic plates analogous to the von Karman plate equation including stretching-bending coupling and in-plane rotatory inertia coupling. Plates considered were cross-ply (0°/90°/0°/90°...) or angle-ply ($\theta/-\theta/\theta/-\theta$...) laminates.

Solutions to the problems of displacements due to transverse and lateral static loadings were presented using trigonometric functions after linearising the general von Karman equations.

The most extensive work on plates of composite materials in one volume is the book by Ashton and Whitney [1] published in 1970.

In 1967 Pagano [6-7-18] included transverse shear deformation in the analysis of a bi-directional composite beam. Pagano published two papers in 1970 [8-9]: one dealing with cylindrical bending and the other with rectangular bidirectional composite layered plates.

By using the F.S.D.T. (*First Shear Deformation Theory*) [12-13], because of different Young's moduli in two adjacent layers, there is a discontinuity of normal stresses at the interface between sheets.

The aim of the present work deals with the nonlinear analysis of laminated composite plates in the case of transverse loadings. The analysis is developed by using a finite element technique based on a shear deformation theory which accounts for the transverse shear also including nonlinear terms in the strain-displacement relationship in the sense of von Karman.

Numerical results are presented giving deflections of square and rectangular plates with various edge boundary conditions.

GOVERNING EQUATIONS OF MODERATELY THICK PLATE MODEL.

The type of plate under discussion consists of n layers of orthotropic sheets bonded together.

The origin of the coordinate system (x, y) is taken in the middle plane Ω of the plate with the z axis perpendicular to it. Each layer has an arbitrary thickness; the elastic properties and the orientation of orthotropic axes of each layer, with respect to the plate axes, are also arbitrary.

It is well-known, from experimental observations, that the Kirchhoff-Love theory of thin plates (in which it is assumed that normals to the midplane before deformation remain straight and normal to the plane after deformation) underpredicts deflections.

These results derive from neglect of transverse shear strains in the classical plate theory. For plates with side-to-thickness ratios greater than 20 the transverse normal and shear stresses are negligible when compared to the remaining stresses.

The inaccuracy of these previous results is faced in this work by using the Mindlin-Reissner plate theory [5-14] in which plane sections originally perpendicular to the middle plane of the plate remain plane, but not necessarily perpendicular to it.

Then, the displacement field is given by:

$$\begin{cases} u(x,y,z) = u_0(x,y) + z\psi_x(x,y) \\ v(x,y,z) = v_0(x,y) + z\psi_y(x,y) \\ w(x,y,z) = w_0(x,y) \end{cases} \tag{1}$$

in which u, v, w are, respectively, the displacements in the x, y, z directions, u_0, v_0, w_0 are the corresponding midplane displacements and ψ_x, ψ_y are the bending slopes in the xz and yz planes.

Assuming that the transverse deflection is comparable to the total thickness of the plate and strains are much smaller than rotations, the nonlinear strain-displacement

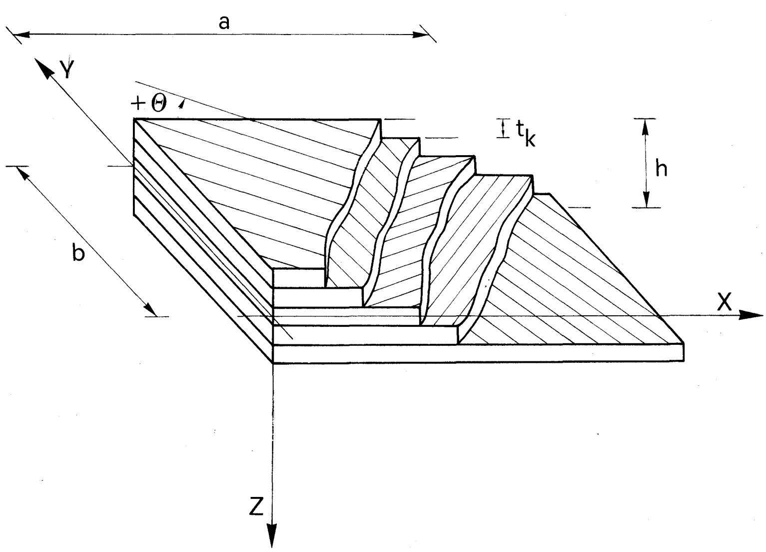

Fig. 1. – Plate model.

relations can be taken as:

$$(2)\qquad \begin{cases} \varepsilon_{xx} = u_{0,x} + \dfrac{1}{2} w_{0,x}^2 + z\psi_{x,x} \\ \varepsilon_{yy} = v_{0,y} + \dfrac{1}{2} w_{0,y}^2 + z\psi_{y,y} \\ \varepsilon_{zz} = \dfrac{1}{2}(\psi_x^2 + \psi_y^2) \\ 2\varepsilon_{xz} = \psi_x + w_{,x} \\ 2\varepsilon_{yz} = \psi_y + w_{,y} \\ 2\varepsilon_{xy} = u_{0,y} + v_{0,x} + w_{0,x} w_{0,y} + z(\psi_{x,y} + \psi_{y,x}) \end{cases}$$

Given that:

$$(3)\qquad \begin{cases} \varepsilon_x^0 = u_{0,x} + \dfrac{1}{2} w_{0,x}^2 \qquad \varepsilon_y^0 = v_{0,y} + \dfrac{1}{2} w_{0,y}^2 \\ \varepsilon_{xy}^0 = u_{0,y} + v_{0,x} + w_{0,x} w_{0,y} \\ \chi_x = \psi_{x,x} \qquad \chi_y = \psi_{y,y} \\ \chi_{xy} = \psi_{y,x} + \psi_{x,y} \qquad \gamma_{xz} = \psi_x + w_{,x} \\ \gamma_{yz} = \psi_y + w_{,y} \end{cases}$$

Then:

$$(4)\qquad \begin{cases} \varepsilon_{xx} = \varepsilon_x^0 + z\chi_x \\ \varepsilon_{yy} = \varepsilon_y^0 + z\chi_y \\ 2\varepsilon_{xy} = \varepsilon_{xy}^0 + z\chi_{xy} \\ 2\varepsilon_{xz} = \gamma_{xz} \\ 2\varepsilon_{yz} = \gamma_{yz} \end{cases}$$

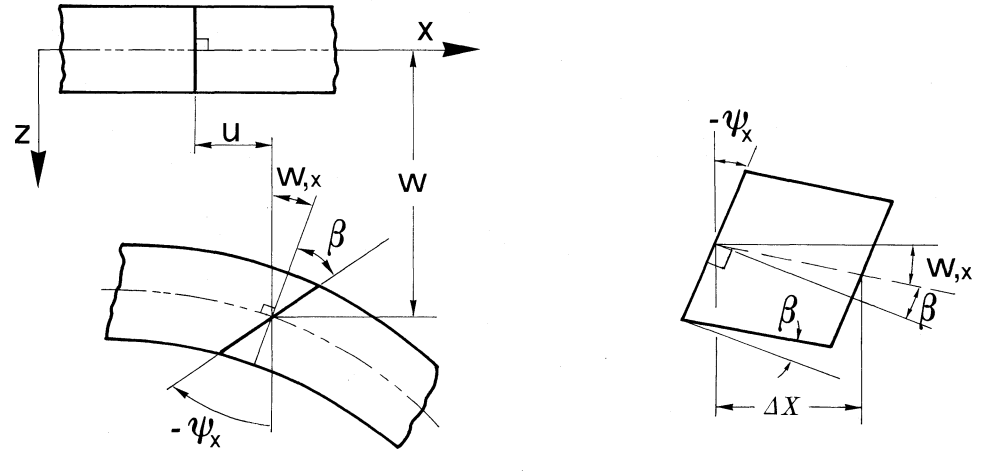

Fig. 2. – Effect of shear deformation (β: slope due to the shear deformation).

Furthermore, ε_{zz} is neglected since the constitutive relations are based on the plane-stress assumption.

With reference to fig. 3, the constitutive equations of the k-th layer are:

$$\left\{\begin{matrix} \bar{\sigma}^k_{11} \\ \bar{\sigma}^k_{22} \\ \bar{\sigma}^k_{12} \\ \bar{\sigma}^k_{13} \\ \bar{\sigma}^k_{23} \end{matrix}\right\} = \begin{bmatrix} \bar{C}^k_{11} & \bar{C}^k_{12} & 0 & 0 & 0 \\ \bar{C}^k_{21} & \bar{C}^k_{22} & 0 & 0 & 0 \\ 0 & 0 & \bar{C}^k_{33} & 0 & 0 \\ 0 & 0 & 0 & \bar{C}^k_{44} & 0 \\ 0 & 0 & 0 & 0 & \bar{C}^k_{55} \end{bmatrix} \left\{\begin{matrix} \bar{\varepsilon}^k_{11} \\ \bar{\varepsilon}^k_{22} \\ \bar{\varepsilon}^k_{12} \\ \bar{\varepsilon}^k_{13} \\ \bar{\varepsilon}^k_{23} \end{matrix}\right\} \tag{5}$$

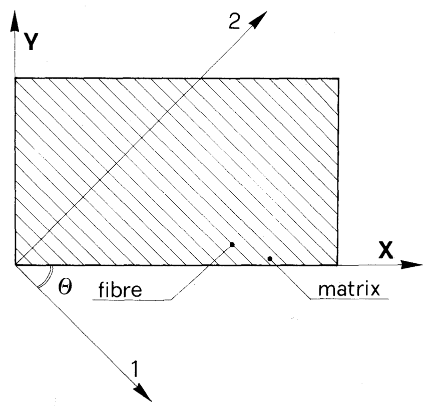

Fig. 3. – Global and natural directions.

where $\bar{\sigma}^k_{ij}$ and $\bar{\varepsilon}^k_{ij}$ are the components of stress and strain tensors, respectively, defined in the material coordinates, and $\bar{C}^k_{ij}$ are the material stiffness coefficients.

The coefficients $\bar{C}^k_{ij} = \bar{C}^k_{ji}$ are given (in terms of engineering constants) by:

$$\begin{cases} \bar{C}^k_{11} = E^k_1/(1 - \nu^k_{12}\,\nu^k_{21}) \\ \bar{C}^k_{12} = \nu^k_{12}\,E^k_2/(1 - \nu^k_{12}\,\nu^k_{21}) \\ \bar{C}^k_{21} = \nu^k_{21}\,E^k_1/(1 - \nu^k_{12}\,\nu^k_{21}) \\ \bar{C}^k_{22} = E^k_2/(1 - \nu^k_{12}\,\nu^k_{21}) \\ \bar{C}^k_{33} = G^k_{12} \qquad \bar{C}^k_{44} = G^k_{13} \qquad \bar{C}^k_{55} = G^k_{23} \end{cases} \tag{6}$$

where G^k_{12}, G^k_{13}, G^k_{23} are layer in-plane and thickness shear moduli and E^k_1, E^k_2 are, respectively, the layer elastic moduli in directions along fibres (direction 1) and normal to them (direction 2).

As a consequence of the symmetry conditions:

$$\nu^k_{12}/E^k_1 = \nu^k_{21}/E^k_2 \tag{7}$$

for which:

$$\nu^k_{21} = \frac{E^k_2}{E^k_1}\,\nu^k_{12} \tag{8}$$

Then, for an orthotropic elastic medium there are only six independent elastic constants, when the constitutive relations are based on the plane-stress assumption.

For k-th layer, the stress-strain relation, with respect to the plate axes x, y, z, is obtained from:

$$\{\sigma^k\} = [T^k][\overline{C}^k][T^k]^{-1}\{\varepsilon^k\} = [C^k]\{\varepsilon^k\} \tag{9}$$

where $\{\sigma^k\}$ and $\{\varepsilon^k\}$ are the components of stress and strain tensors defined with reference to the plate axes.

$$\{\sigma^k\} = \begin{Bmatrix} \sigma_x^k \\ \sigma_y^k \\ \tau_{xy}^k \\ \tau_{xz}^k \\ \tau_{yz}^k \end{Bmatrix}; \qquad \{\varepsilon^k\} = \begin{Bmatrix} \varepsilon_x^k \\ \varepsilon_y^k \\ 2\varepsilon_{xy}^k \\ 2\varepsilon_{xz}^k \\ 2\varepsilon_{yz}^k \end{Bmatrix} \tag{10}$$

The transformation matrix T^k is given by:

$$[T^k] = \begin{bmatrix} A^k & B^k & 2C^k & 0 & 0 \\ B^k & A^k & -2C^k & 0 & 0 \\ -C^k & C^k & D^k & 0 & 0 \\ 0 & 0 & 0 & m^k & n^k \\ 0 & 0 & 0 & -n^k & m^k \end{bmatrix} \tag{11}$$

in which:

$$\begin{cases} m^k = \cos\theta^k & n^k = \operatorname{sen}\theta^k & A^k = \cos^2\theta^k \\ B^k = \operatorname{sen}^2\theta^k & C^k = \operatorname{sen}\theta^k\cos\theta^k & D^k = \cos^2\theta^k - \operatorname{sen}^2\theta^k \end{cases} \tag{12}$$

The coefficients C_{ij}^k are given by:

$$\begin{cases} C_{11}^k = \overline{C}_{11}^k\cos^4\theta^k + 2(\overline{C}_{12}^k + 2\overline{C}_{33}^k)\cos^2\theta^k\operatorname{sen}^2\theta^k + \overline{C}_{22}^k\operatorname{sen}^4\theta^k \\ C_{12}^k = (\overline{C}_{11}^k + \overline{C}_{22}^k - 4\overline{C}_{33}^k)\operatorname{sen}^2\theta^k\cos^2\theta^k + \overline{C}_{12}^k(\operatorname{sen}^4\theta^k + \cos^4\theta^k) \\ C_{13} = (-\overline{C}_{11}^k + \overline{C}_{12}^k + 2\overline{C}_{33}^k)\operatorname{sen}\theta^k\cos^3\theta^k + (-\overline{C}_{12}^k + \overline{C}_{22}^k - 2\overline{C}_{33}^k)\operatorname{sen}^3\theta^k\cos\theta^k \\ C_{22} = \overline{C}_{11}^k\operatorname{sen}^4\theta^k + 2(\overline{C}_{12}^k + 2\overline{C}_{33}^k)\operatorname{sen}^2\theta^k\cos^2\theta^k + \overline{C}_{22}^k\cos^4\theta^k \\ C_{31}^k = C_{13}^k \qquad C_{21}^k = C_{12}^k \qquad C_{32}^k = C_{23}^k \qquad C_{54}^k = C_{45}^k \\ C_{33}^k = (\overline{C}_{11}^k + \overline{C}_{22}^k - 2\overline{C}_{12}^k - 2\overline{C}_{33}^k)\operatorname{sen}^2\theta^k\cos^2\theta^k + \overline{C}_{33}^k(\operatorname{sen}^4\theta^k + \cos^4\theta^k) \\ C_{23}^k = (-\overline{C}_{11}^k + \overline{C}_{12}^k + 2\overline{C}_{33}^k)\operatorname{sen}^3\theta^k\cos\theta^k(-\overline{C}_{12}^k + \overline{C}_{22}^k - 2\overline{C}_{33}^k)\operatorname{sen}\theta^k\cos^3\theta^k \\ C_{44}^k = G_{13}^k\cos^2\theta^k + G_{23}^k\operatorname{sen}^2\theta^k \\ C_{45}^k = (G_{23}^k - G_{13}^k)\operatorname{sen}\theta^k\cos\theta^k \\ C_{55}^k = G_{13}^k\operatorname{sen}^2\theta^k + G_{23}^k\cos^2\theta^k \end{cases} \tag{13}$$

The total potential energy of the plate, in absence of body forces and neglecting both body moments and surface shearing forces, is given by:

$$\Pi = U + V \tag{14}$$

where:

$$U = \frac{1}{2}\int_V \sigma\,\varepsilon\,dV = \frac{1}{2}\int_\Omega \sum_{k=1}^{n}\int_{h_{k-1}}^{h_k} (\sigma_x^k\,\varepsilon_{xx}^k + \sigma_y\,\varepsilon_{yy}^k + 2\tau_{xy}\,\varepsilon_{xy}^k + 2\tau_{xz}^k\,\varepsilon_{xz}^k + 2\tau_{yz}^k\,\varepsilon_{yz}^k)\,dz\,d\Omega \tag{15}$$

$$\begin{aligned} V = &- \int_\Omega q_0 W\,d\Omega - \int_{C_1} \overline{N}_n u_n\,dC_1 - \int_{C_2} \overline{N}_s u_s\,dC_2 + \\ &- \int_{C_3} \overline{M}_n \psi_n\,dC_3 - \int_{C_4} \overline{M}_s \psi_s\,dC_4 - \int_{C_5} \overline{Q}_n w\,dC_5 \end{aligned} \tag{16}$$

C_1, C_2, C_3, C_4, C_5 are, respectively, the (possibly overlapping) portions of the boundary on which N_n, N_s, M_n, M_s, Q_n are specified.

It is helpful to define the stress and moment resultants as follows:

$$\begin{cases} N_x = \sum_{k=1}^{n}\int_{h_{k-1}}^{h_k} \sigma_x^k\,dz\,; \quad N_y = \sum_{k=1}^{n}\int_{h_{k-1}}^{h_k} \sigma_y^k\,dz\,; \\ M_x = \sum_{k=1}^{n}\int_{h_{k-1}}^{h_k} \sigma_x^k z\,dz\,; \quad M_y = \sum_{k=1}^{n}\int_{h_{k-1}}^{h_k} \sigma_y^k z\,dz\,; \\ N_{xy} = N_{yx} = \sum_{k=1}^{n}\int_{h_{k-1}}^{h_k} \tau_{xy}^k\,dz\,; \quad M_{xy} = M_{yx} = \sum_{k=1}^{n}\int_{h_{k-1}}^{h_k} \tau_{xy}^k z\,dz\,; \\ Q_x = \sum_{k=1}^{n}\int_{h_{k-1}}^{h_k} \tau_{xz}^k\,dz\,; \quad Q_y = \sum_{k=1}^{n}\int_{h_{k-1}}^{h_k} \tau_{yz}^k\,dz\,. \end{cases} \tag{17}$$

The symbols h_k and h_{k-1} denote, respectively, the distances from the midplane to the lower and upper surface of the k-th layer.

The solution to the problem can be reached by using a variational form of the total potential energy functional.

Therefore, by taking into account the relations (17) and (2, 3, 4), the stationary condition to this functional gives:

$$\begin{aligned} \delta\Pi = \int_\Omega (N_x\,\delta\varepsilon_x^0 + N_y\,\delta\varepsilon_y^0 + N_{xy}\,\delta\varepsilon_{xy}^0 + M_x\,\delta\chi_x + M_y\,\delta\chi_y + M_{xy}\,\delta\chi_{xy} + \\ + Q_x\,\delta\chi_{xz} + Q_y\,\delta\chi_{yz} - q_0\delta w)\,d\Omega - \int_{C_1} \overline{N}_n\,\delta u_n\,dC_1 - \int_{C_2} \overline{N}_s\,\delta u_s\,dC_2 + \\ - \int_{C_3} \overline{M}_n\,\delta\psi_n\,dC_3 - \int_{C_4} \overline{M}_s\,\delta\psi_s\,dC_4 - \int_{C_5} \overline{Q}_n\,\delta w\,dC_5 = 0\,. \end{aligned} \tag{18}$$

On the other hand, eq. (18), by using the virtual displacements principle, becomes:

$$\begin{aligned} \delta\Pi = \int_\Omega \Bigg\{ \left(\mathcal{N} + \frac{\partial Q_x}{\partial x} + \frac{\partial Q_y}{\partial y} - q_0\right)\delta w + \left(\frac{\partial N_x}{\partial x} + \frac{\partial N_{xy}}{\partial y}\right)\delta u + \\ + \left(\frac{\partial N_y}{\partial y} + \frac{\partial N_{xy}}{\partial x}\right)\delta v + \left(\frac{\partial M_x}{\partial x} + \frac{\partial M_{xy}}{\partial y} - Q_x\right)\delta\psi_x + \left(\frac{\partial M_y}{\partial y} + \frac{\partial M_{xy}}{\partial x} - Q_y\right)\delta\psi_y \Bigg\}\,d\Omega = 0 \end{aligned} \tag{19}$$

where:

$$\mathcal{N} = \frac{\partial}{\partial x}\left(N_x \frac{\partial w}{\partial x}\right) + \frac{\partial}{\partial y}\left(N_y \frac{\partial w}{\partial y}\right) + \frac{\partial}{\partial x}\left(N_{xy} \frac{\partial w}{\partial y}\right) + \frac{\partial}{\partial y}\left(N_{xy} \frac{\partial w}{\partial x}\right).$$

Now, the following matrices can be defined:

$$(20)\quad \begin{cases} A_{ij} = \sum_{k=1}^{n} \int_{h_{k-1}}^{h_k} C_{ij}^k\, dz = \sum_{k=1}^{n} C_{ij}^k (h_k - h_{k-1}) \\ \qquad (i,j = 1,2,3) \quad \text{(Extensional stiffness)}; \\ B_{ij} = \sum_{k=1}^{n} \int_{h_{k-1}}^{h_k} C_{ij}^k z\, dz = \frac{1}{2} \sum_{k=1}^{n} C_{ij}^k (h_k^2 - h_{k-1}^2) \\ \qquad (i,j = 1,2,3) \quad \text{(Flexural-extensional stiffness)}; \\ D_{ij} = \sum_{k=1}^{n} \int_{h_{k-1}}^{h_k} C_{ij}^k z^2\, dz = \frac{1}{3} \sum_{k=1}^{n} C_{ij}^k (h_k^3 - h_{k-1}^3) \\ \qquad (i,j = 1,2,3) \quad \text{(Flexural stiffness)}; \\ H_{ij} = K^2 \sum_{k=1}^{n} \int_{h_{k-1}}^{h_k} C_{ij}^k\, dz = K^2 \sum_{k=1}^{n} C_{ij}^k (h_k - h_{k-1}) \\ \qquad (i,j = 4,5) \quad \text{(Thickness shear stiffness)}. \end{cases}$$

where $K^2 = 5/6$ is the square of the shear correction coefficient [5].

Combining eq. (20) with relations (9), (10), (17) and (4) the following plate constitutive equations are obtained:

$$(21)\quad \{\boldsymbol{N}\} = [\boldsymbol{A}]\{\varepsilon_0\} + [\boldsymbol{B}]\{\chi\}$$

$$(22)\quad \{\boldsymbol{M}\} = [\boldsymbol{B}]\{\varepsilon_0\} + [\boldsymbol{D}]\{\chi\}$$

$$(23)\quad \begin{Bmatrix} Q_x \\ Q_y \end{Bmatrix} = \begin{bmatrix} H_{44} & H_{45} \\ H_{54} & H_{55} \end{bmatrix} \begin{Bmatrix} \gamma_{xz} \\ \gamma_{yz} \end{Bmatrix}$$

where:

$$(24)\quad \{\boldsymbol{N}\} = \begin{Bmatrix} N_x \\ N_y \\ N_{xy} \end{Bmatrix}; \qquad \{\boldsymbol{M}\} = \begin{Bmatrix} M_x \\ M_y \\ M_{xy} \end{Bmatrix}$$

$$(25)\quad \{\varepsilon_0\} = \begin{Bmatrix} \varepsilon_x^0 \\ \varepsilon_y^0 \\ \varepsilon_{xy}^0 \end{Bmatrix}; \qquad \{\chi\} = \begin{Bmatrix} \chi_x \\ \chi_y \\ \chi_{xy} \end{Bmatrix}.$$

Finite element formulation.

In this section a finite element model based on the variational formulation of the equation (18) is presented.

The region Ω is divided into a finite number of isoparametric rectangular elements [10, 11].

Over each element the generalized displacements (u, v, w, ψ_x, ψ_y) are interpolated by:

$$\tag{26} \begin{cases} u = \sum_{i=1}^{N} u_i f_i; \quad v = \sum_{i=1}^{N} v_i f_i; \quad w = \sum_{i=1}^{N} w_i f_i; \\ \psi_x = \sum_{i=1}^{N} \psi_{xi} f_i; \quad \psi_y = \sum_{i=1}^{N} \psi_{yi} f_i; \end{cases}$$

where u_i, v_i, w_i, ψ_{xi}, ψ_{yi} are the values of the unknown functions at the global nodes of the mesh and f_i are the interpolation functions.

The substitution of relations (26) into eq. (18) gives:

$$\tag{27} \boldsymbol{K}\boldsymbol{U} = \boldsymbol{F}$$

where $\boldsymbol{U}$ collects the nodal values of the generalized displacements u, v, w, ψ_x, ψ_y; $\boldsymbol{K}$ is the stiffness matrix of the plate, and $\boldsymbol{F}$ is the nodal force vector.

It should be observed that the stiffness matrik $\boldsymbol{K}$ depends on the solution $\boldsymbol{U}$. Therefore, a standard iterative procedure must be used.

The coefficients of the stiffness matrix $\boldsymbol{K}$ (secant) are given in the appendix.

NUMERICAL RESULTS AND CONCLUDING REMARKS.

In this section the formulations obtained above are used in the nonlinear analysis of square and rectangular moderately thick plates.

Tables I and II contain, respectively, a list of the materials and the boundary condition considered here.

Plates are subject to a uniformly distributed load applied on the top surface and acting in direction z.

In all computations a mesh of (3×3) nine-node quadratic elements is used.

It should be observed that no noticeable effect of the integration of shear terms is found in calculations for the quadratic elements used.

Fig. 4 shows the ratio between the centre deflection obtained using the shear deformation theory and that obtained using the classical thin plate theory *vs.* the side-to-thickness ratio.

This is given for an isotropic plate, two layer and eight layer cross-ply square laminates, subject to a uniform load.

The plate boundary conditions here considered are SS1 (*simply supported*).

TABLE I. – *Mechanical properties of laminae.*

MATERIAL	E_1/E_2	G_{12}/E_2	G_{13}/E_2	G_{23}/E_2	ν_{12}
BORON EPOXY	10.0	0.333	0.333	0.333	0.22
GRAPHITE EPOXY	40.0	0.5	0.5	0.5	0.25
GLASS EPOXY	3.0	0.5	0.5	0.5	0.25
MATERIAL I	25.0	0.5	0.5	0.2	0.25

TABLE II. – *Boundary conditions.*

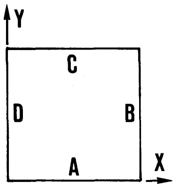

	SIDE A	SIDE B	SIDE C	SIDE D
SS1	$u, w, \psi_x = 0$	$v, w, \psi_y = 0$	$u, w, \psi_x = 0$	$v, w, \psi_y = 0$
CC2	$u, v, w, \psi_x = 0$	$u, v, w, \psi_y = 0$	$u, v, w, \psi_x = 0$	$u, v, w, \psi_y = 0$
CC1	all edges clamped: $u, v, w, \psi_x, \psi_y = 0$			
SC	$u, w, \psi_x = 0$	$u, v, w, \psi_x, \psi_y = 0$	$u, w, \psi_x = 0$	$u, v, w, \psi_x, \psi_y = 0$
CSCS	$w, \psi_y = 0$	$v, w, \psi_y = 0$	$w, \psi_y = 0$	$v, w, \psi_y = 0$

The orthotropic layers are made of *material I*; the isotropic plate has: $E = E_2$ and $G = E/(2(1 + \nu_{12}))$.

The influence of shear deformability on bending is extremely relevant when $a/h \leq 20$.

The results above reaffirm the importance of including shear deformation in laminated composite structures.

Fig. 5 plots the nondimensional transverse centre deflection W_c/h *vs.* the analysis of nondimensional transverse load $\bar{q} = (q_0/E_2)(a/h)^4$ of a simply supported (SS1) square cross-ply plate [2].

Again, the layers are made of *material I.*

It should be observed that deflections are overestimated if a linear analysis is carried

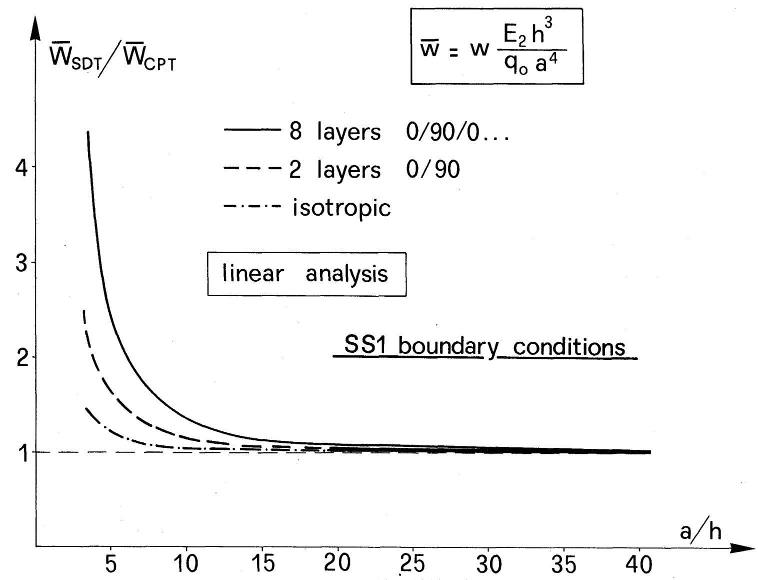

Fig. 4. – Effect of shear deformability.

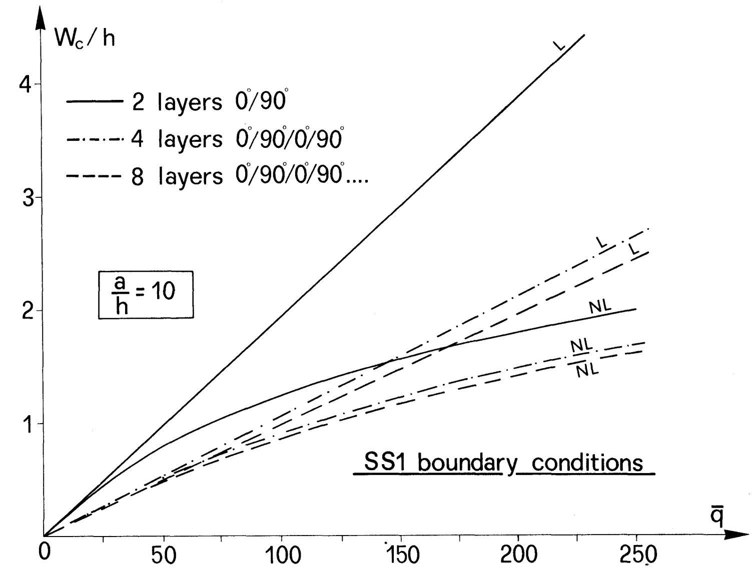

Fig. 5. – Transverse centre deflection W_c/h *v/s* load $\bar{q} = (q_0/E_2)(a/b)^4$ influence of layering on deformability. (L = linear, NL = nonlinear).

out; however the difference between the linear and nonlinear solution decreases with layering.

A cursory examination of (20) reveals that the coupling between bending and stretching as displayed in eqs. (21) (22) vanishes as the number of layers increases.

Figs. 6*a, b, c* show the nondimensional centre deflection of n-layer square plates made of Graphite-Expoxy material *vs.* angle θ for various boundary conditions [15].

When the number of layers is high ($n \geq 6 \div 7$) the «uncoupled» solution is reached.

A vast difference can be observed between results relative to the linear and nonlinear analysis, especially when coupled behaviour takes place.

For the SS1 boundary conditions (fig. 6*a*), the linear analysis, in the case of two layers, shows rigidity at a maximum when $\theta = 0°$ and $\theta = 45°$ and a minimum when $\theta \cong 12.5°$.

On the other hand the nonlinear analysis gives a single optimal value of $\theta = 45°$.

However, if there are 4 or more layers (even up to and beyond 100) the linear solution is similar to the nonlinear one (with the minimum rigidity when $\theta = 0°$, and the maximum when $\theta = 45°$).

In fig. 6*c*, relative to the clamped scheme, it can be noted that, in the linear analysis, a plate manufactured with 2 layers has the maximum rigidity when $\theta = 0°$.

For 4 layers and more the angle of minimum deflection is $\theta = 45°$.

The nonlinear analysis shows a single optimal $\theta = 0°$ for all types of plates.

The same behaviour seen in fig. 6*c* can be also be observed in fig. 6*b* which represents the *SC* boundary conditions.

Fig. 7 plots the nondimensional transverse centre deflection W_c/h versus the E_1/E_2 ratio of a simply supported (SS1) cross-ply square plate.

In these calculi $G_{12} = G_{13} = G_{23} = 0.5E_2$; and $\nu_{12} = 0.25$ were assumed.

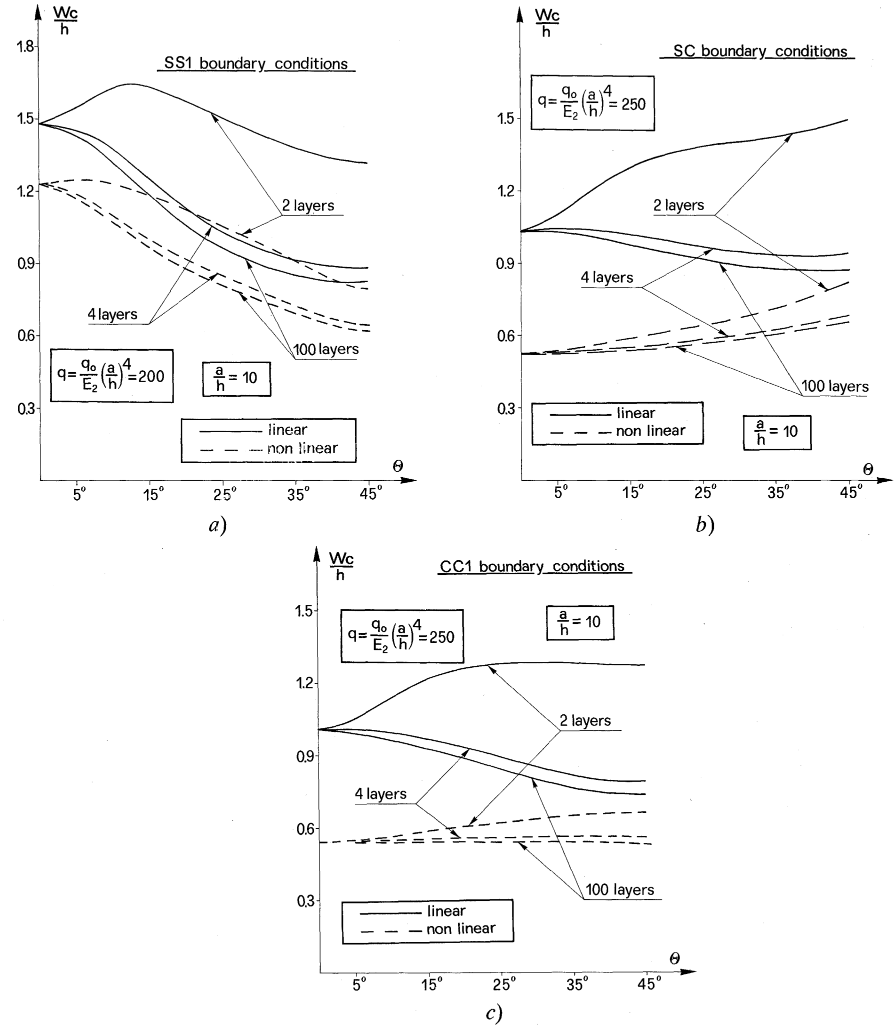

Fig. 6*a*, *b*, *c*. – Effect of fibre orientation on centre deflection of angle-ply square plates under various boundary conditions.

In particular the diagrams show the dependence of the coupling effect on the ratio E_1/E_2.

A sufficiently high transverse nondimensional load ($\overline{q} = (q_0/E_2)(a/h)^4 = 50$) was assumed, so that nonlinear behaviour would have an appreciable effect.

The influence of shear deformability on nonlinear bending is shown, in the same fig. 7, by the comparison between results relative to both ratios $a/h = 100$ and $a/h = 10$.

In particular the classical plate theory (simulated by $a/h = 100$) underpredicts deflections even at lower ratios of moduli.

Fig. 8 shows the variation of the nondimensional centre deflection *vs.* the a/b ratio.

Plates are in Graphite-Epoxy material. It should be observed that the influence of coupling may be extremely relevant; nevertheless, the centre deflection rapidly reaches the uncoupled solution as the number of layers increases.

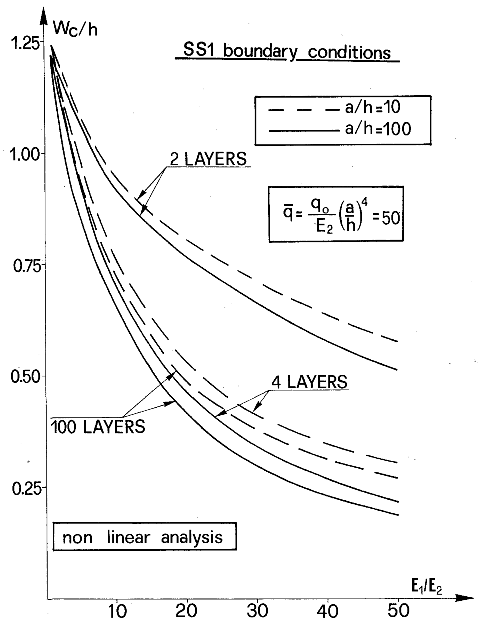

Fig. 7.

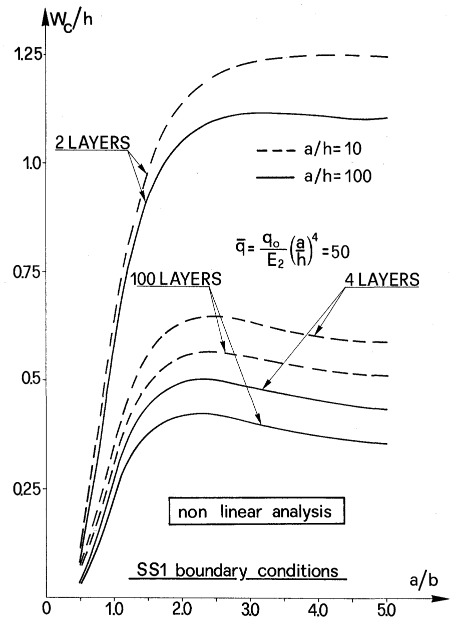

Fig. 8.

Fig. 7. – Effect of material anisotropy on the nondimensional centre deflections of cross-ply laminates under a uniform transverse load for different *a/h* ratios.

Fig. 8. – Centre deflections *v/s a/b* ratio and *a/h* ratio for a square cross-ply plate under a uniform transverse load.

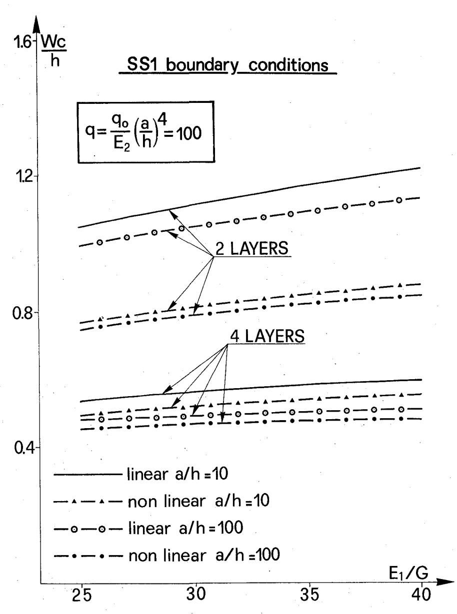

Fig. 9. – Centre deflections as a function of E_1/G ratio for square cross-ply plate under a uniform transverse load.

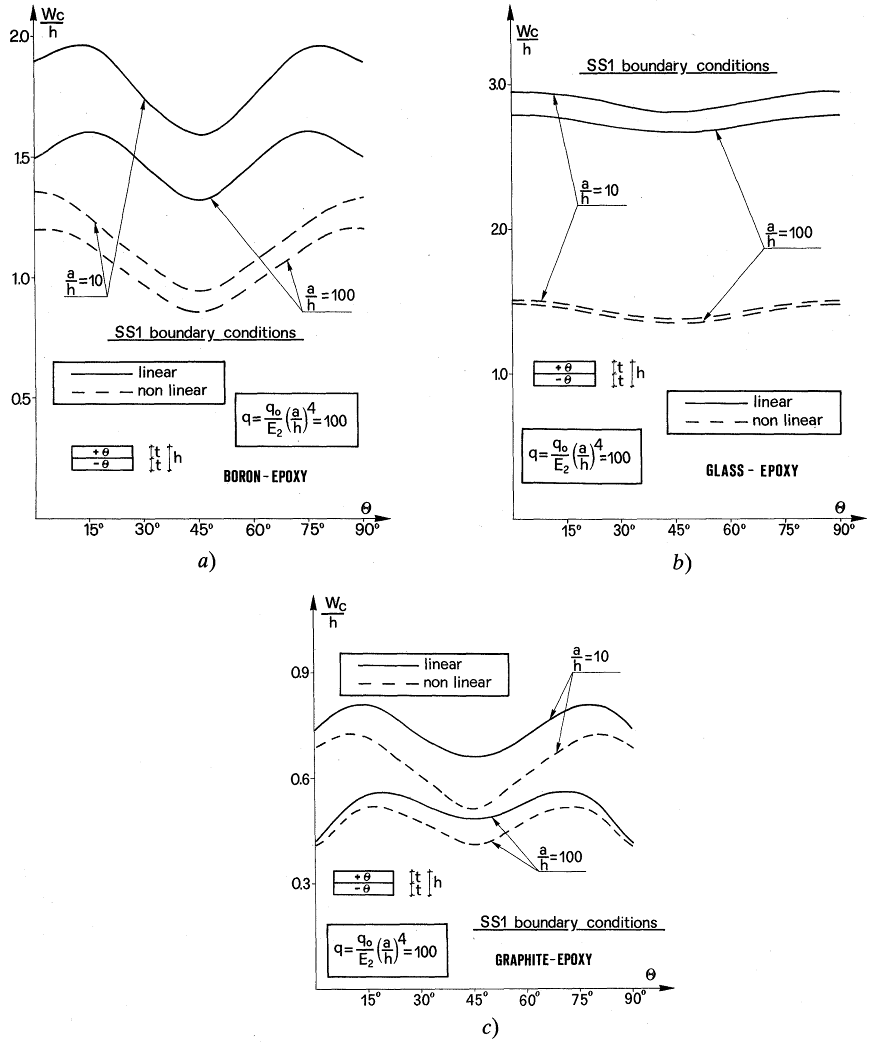

Fig. 10*a, b, c.* – 2-layer angle-ply plate: W_c/h versus angle θ.

Furthermore, when the a/b ratio increases, the W_c/h ratio becomes asymptotic, with different values for each type of laminate.

Fig. 9 shows the nondimensional centre deflections *vs.* the E_1/G ratio of a square cross-ply plate under SS1 boundary conditions.

The material considered has the following mechanical properties:

$$E_1/E_2 = 40;\ \nu_{12} = 0.25;\ G = G_{12} = G_{13} = G_{23}.$$

An almost linear increase of deflections is noted with the increase of the E_1/G ratio.

The results relative to the plate manufactured with two layers show a large difference between the results of both linear and nonlinear analysis when $a/h = 10$ and $a/h = 100$.

This difference is lower for a 4 layer plate which has an uncoupled behaviour.

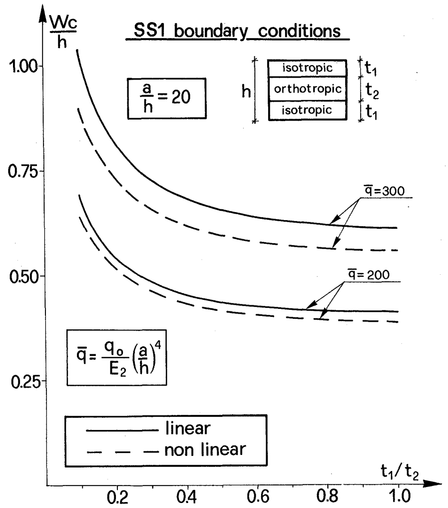

a)

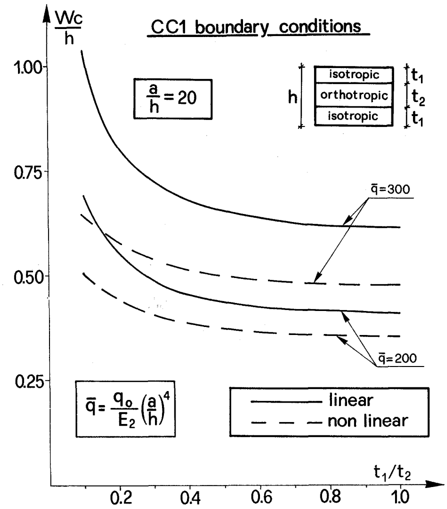

b)

Fig. 11*a, b*. – 3-layer sandwich plate: influence of thickness ratio t_1/t_2 on the maximum deflection W_c/h.

Figs. 10*a, b, c* show the variation of the centre deflection, W_c/h, versus the fibre orientation of an angle-ply square composite plate made with various materials.

Two values of the a/h ratio are considered; furthermore only the simply supported boundary conditions is analysed.

A clear difference between linear and nonlinear analysis can be observed, especially for the plate made of Glass-Epoxy.

In particular, for all materials (except Graphite-Epoxy in the linear analysis with $a/h = 100$), the linear and nonlinear solutions give an optimal value of $\theta = 45°$.

In figs. 11*a, b* the effect of the thickness ratio t_1/t_2 on the deformability of a 3-layer square plate with an orthotropic core, under the SS1 and CC1 boundary conditions, is shown for different values of load $\overline{q}$.

The orthotropic core is made of *material I*; for the isotropic layers we assumed:

$$E = E_1; \qquad G = E/(2\,(1 + \nu_{12})); \qquad \nu_{12} = 0.25\,.$$

It can be observed that the linear and nonlinear deflections decrease with t_1/t_2.

Finally figs. 12*a, b* show the nondimensional centre deflection *vs.* the b/a ratio for CC1 boundary conditions and for different values of load $\overline{q} = (q_0/E_2)(a/h)^4$.

In particular in the case of fig. 12*a* the orthotropic core has the fibre direction perpendicular to the shorter side (modulus E_1).

This plate has a higher rigidity than the analogous plate with the core fibre orientation parallel to the major side.

A greater difference between linear and nonlinear solutions can be observed in fig. 12*b*.

In any case this difference is more pronounced when the b/a ratio increases.

Acknowledgement. The authors of this work gratefully acknowledge the financial support of the Italian Ministry of Education (M.P.I. 60% quota).

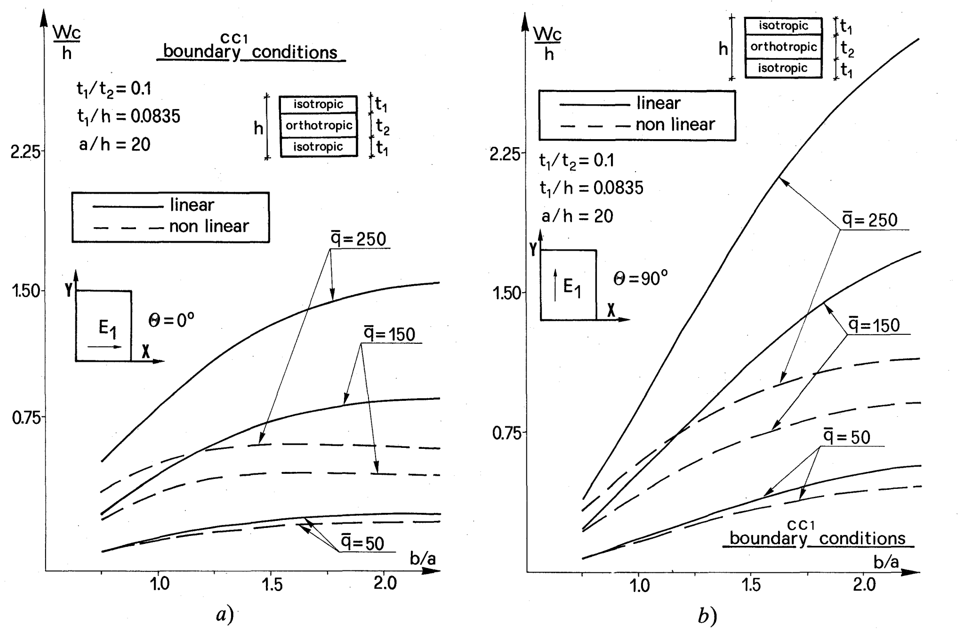

Fig. 12*a, b*. – 3-layer sandwich plate: influence of the aspect ratio on the maximum deflection W_c/h.

Appendix

Coefficients of the secant stiffness matrix ***K***

$$\begin{bmatrix} K^{L}_{11}+K^{NL}_{11} & K^{L}_{12}+K^{NL}_{12} & K^{L}_{13}+K^{NL}_{13} & K^{NL}_{14} & K^{NL}_{15} \\ K^{L}_{21}+K^{NL}_{21} & K^{L}_{22} & K^{L}_{23} & K^{L}_{24} & K^{L}_{25} \\ K^{L}_{31}+K^{NL}_{31} & K^{L}_{32} & K^{L}_{33} & K^{L}_{34} & K^{L}_{35} \\ K^{NL}_{41} & K^{L}_{42} & K^{L}_{43} & K^{L}_{44} & K^{L}_{45} \\ K^{NL}_{51} & K^{L}_{52} & K^{L}_{53} & K^{L}_{54} & K^{L}_{55} \end{bmatrix}$$

linear coefficients

$$K^{L}_{11} = \int_{\Omega} (H_{44}\, w_{,x}\, \delta w_{,x} + H_{45}\, w_{,y}\, \delta w_{,x} + H_{54}\, w_{,x}\, \delta w_{,y} + H_{55}\, w_{,y}\, \delta w_{,y})\, dx\, dy$$

$$K^{L}_{12} = \int_{\Omega} (H_{44}\, \psi_x\, \delta w_{,x} + H_{54}\, \psi_x\, \delta w_{,y})\, dx\, dy$$

$$K^{L}_{13} = \int_{\Omega} (H_{45}\, \psi_y\, \delta w_{,x} + H_{55}\, \psi_y\, \delta w_{,y})\, dx\, dy$$

$$K^{L}_{21} = \int_{\Omega} (H_{44}\, w_{,x}\, \delta\psi_x + H_{45}\, w_{,y}\, \delta\psi_x)\, dx\, dy$$

$$K^{L}_{22} = \int_{\Omega} (H_{44}\, \psi_x\, \delta\psi_x + D_{11}\, \psi_{x,x}\, \delta\psi_{x,x} + D_{13}\, \psi_{x,y}\, \delta\psi_{x,x} + D_{31}\, \psi_{x,x}\, \delta\psi_{x,y} + D_{33}\, \psi_{x,y}\, \delta\psi_{x,y})\, dx\, dy$$

$$K^{L}_{23} = \int_{\Omega} (H_{45}\, \psi_y\, \delta\psi_x + D_{12}\, \psi_{y,y}\, \delta\psi_{x,x} + D_{13}\, \psi_{y,x}\, \delta\psi_{x,x} + D_{32}\, \psi_{y,y}\, \delta\psi_{x,y} + D_{33}\, \psi_{y,x}\, \delta\psi_{x,y})\, dx\, dy$$

$$K^{L}_{24} = \int_{\Omega} (B_{11}\, u_{,x}\, \delta\psi_{x,x} + B_{13}\, u_{,y}\, \delta\psi_{x,x} + B_{31}\, u_{,x}\, \delta\psi_{x,y} + B_{33}\, u_{,y}\, \delta\psi_{x,y})\, dx\, dy$$

$$K^{L}_{25} = \int_{\Omega} (B_{12}\, v_{,y}\, \delta\psi_{x,x} + B_{13}\, v_{,x}\, \delta\psi_{x,x} + B_{32}\, v_{,y}\, \delta\psi_{x,y} + B_{33}\, v_{,x}\, \delta\psi_{x,y})\, dx\, dy$$

$$K^{L}_{31} = \int_{\Omega} (H_{54}\, w_{,x}\, \delta\psi_{y} + H_{55}\, w_{,y}\, \delta\psi_{y})\, dx\, dy$$

$$K^{L}_{32} = \int_{\Omega} (D_{21}\, \psi_{x,x}\, \delta\psi_{y,y} + D_{23}\, \psi_{x,y}\, \delta\psi_{y,y} + D_{31}\, \psi_{x,x}\, \delta\psi_{y,x} + H_{54}\, \psi_{x}\, \delta\psi_{y} + D_{33}\, \psi_{x,y}\, \delta\psi_{y,x})\, dx\, dy$$

$$K^{L}_{33} = \int_{\Omega} (H_{55}\, \psi_{y}\, \delta\psi_{y} + D_{22}\, \psi_{y,y}\, \delta\psi_{y,y} + D_{23}\, \psi_{y,x}\, \delta\psi_{y,y} + D_{32}\, \psi_{y,y}\, \delta\psi_{y,x} + D_{33}\, \psi_{y,x}\, \delta\psi_{y,x})\, dx\, dy$$

$$K^{L}_{34} = \int_{\Omega} (B_{21}\, u_{,x}\, \delta\psi_{y,y} + B_{23}\, u_{,y}\, \delta\psi_{y,y} + B_{31}\, u_{,x}\, \delta\psi_{y,x} + B_{33}\, u_{,y}\, \delta\psi_{y,x})\, dx\, dy$$

$$K^{L}_{35} = \int_{\Omega} (B_{22}\, v_{,y}\, \delta\psi_{y,y} + B_{23}\, v_{,x}\, \delta\psi_{y,y} + B_{32}\, v_{,y}\, \delta\psi_{y,x} + B_{33}\, v_{,x}\, \delta\psi_{y,x})\, dx\, dy$$

$$K^{L}_{42} = \int_{\Omega} (B_{11}\, \psi_{x,x}\, \delta u_{,x} + B_{13}\, \psi_{x,y}\, \delta u_{,x} + B_{31}\, \psi_{x,x}\, \delta u_{,y} + B_{33}\, \psi_{x,y}\, \delta u_{,y})\, dx\, dy$$

$$K^{L}_{43} = \int_{\Omega} (B_{12}\, \psi_{y,y}\, \delta u_{,x} + B_{13}\, \psi_{y,x}\, \delta u_{,x} + B_{32}\, \psi_{y,y}\, \delta u_{,y} + B_{33}\, \psi_{y,x}\, \delta u_{,y})\, dx\, dy$$

$$K^{L}_{44} = \int_{\Omega} (A_{11}\, u_{,x}\, \delta u_{,x} + A_{13}\, u_{,y}\, \delta u_{,x} + A_{31}\, u_{,x}\, \delta u_{,y} + A_{33}\, u_{,y}\, \delta u_{,y})\, dx\, dy$$

$$K^{L}_{45} = \int_{\Omega} (A_{12}\, v_{,y}\, \delta u_{,x} + A_{13}\, v_{,x}\, \delta u_{,x} + A_{32}\, v_{,x}\, \delta u_{,y} + A_{33}\, u_{,x}\, \delta u_{,y})\, dx\, dy$$

$$K^{L}_{52} = \int_{\Omega} (B_{21}\, \psi_{x,x}\, \delta v_{,y} + B_{23}\, \psi_{x,y}\, \delta v_{,y} + B_{31}\, \psi_{x,x}\, \delta v_{,x} + B_{33}\, \psi_{x,y}\, \delta v_{,x})\, dx\, dy$$

$$K^{L}_{53} = \int_{\Omega} (B_{22}\, \psi_{y,y}\, \delta v_{,y} + B_{23}\, \psi_{y,x}\, \delta v_{,y} + B_{32}\, \psi_{y,y}\, \delta v_{,x} + B_{33}\, \psi_{y,x}\, \delta v_{,x})\, dx\, dy$$

$$K^{L}_{54} = \int_{\Omega} (A_{21}\, u_{,x}\, \delta v_{,y} + A_{23}\, u_{,y}\, \delta v_{,y} + A_{31}\, u_{,x}\, \delta v_{,x} + A_{33}\, u_{,y}\, \delta v_{,x})\, dx\, dy$$

$$K^{L}_{55} = \int_{\Omega} (A_{22}\, v_{,y}\, \delta v_{,y} + A_{23}\, u_{,x}\, \delta v_{,y} + A_{32}\, v_{,y}\, \delta v_{,x} + A_{33}\, v_{,x}\, \delta v_{,x})\, dx\, dy$$

nonlinear coefficients

$$\begin{aligned} K^{NL}_{11} = \int_{\Omega} \Big(& \frac{1}{2} w^2_{,x} (A_{11}\, w_{,x}\, \delta w_{,x} + A_{31}\, w_{,y}\, \delta w_{,x} + 2A_{13}\, w_{,y}\, \delta w_{,x} + A_{21}\, w_{,y}\, \delta w_{,y} + A_{31}\, w_{,x}\, \delta w_{,y} + 2A_{33}\, w_{,y}\, \delta w_{,y}) + \\ & + \frac{1}{2} w^2_{,y} (A_{12}\, w_{,x}\, \delta w_{,x} + A_{22}\, w\, ,y\, \delta w_{,y} + 2A_{23}\, w_{,x}\, \delta w_{,y} + A_{32}\, w_{,x}\, \delta w_{,y} + 2A_{33}\, w_{,x}\, \delta w_{,x} + A_{32}\, w_{,y}\, \delta w_{,x}) \Big)\, dx\, dy \end{aligned}$$

$$\begin{aligned} K^{NL}_{12} = \int_{\Omega} (& w_{,y} (B_{21}\, \psi_{x,x}\, \delta w_{,y} + B_{23}\, \psi_{x,y}\, \delta w_{,y} + B_{31}\, \psi_{x,x}\, \delta w_{,x} + B_{33}\, \psi_{x,y}\, \delta w_{,x}) + \\ & + w_{,x} (B_{31}\, \psi_{x,x}\, \delta w_{,y} + B_{33}\, \psi_{x,y}\, \delta w_{,y} + B_{11}\, \psi_{x,x}\, \delta w_{,x} + B_{13}\, \psi_{x,y}\, \delta w_{,x}))\, dx\, dy \end{aligned}$$

$$\begin{aligned} K^{NL}_{13} = \int_{\Omega} (& w_{,x} (B_{12}\, \psi_{y,y}\, \delta w_{,x} + B_{13}\, \psi_{y,x}\, \delta w_{,x} + B_{32}\, \psi_{y,y}\, \delta w_{,y} + B_{33}\, \psi_{y,x}\, \delta w_{,y}) + \\ & + w_{,y} (B_{22}\, \psi_{y,y}\, \delta w_{,y} + B_{23}\, \psi_{y,x}\, \delta w_{,y} + B_{32}\, \psi_{y,y}\, \delta w_{,x} + B_{33}\, \psi_{y,x}\, \delta w_{,x}))\, dx\, dy \end{aligned}$$

$$\begin{aligned} K^{NL}_{14} = \int_{\Omega} (& w_{,x} (A_{11}\, u_{,x}\, \delta w_{,x} + A_{13}\, u_{,y}\, \delta w_{,x} + A_{31}\, u_{,x}\, \delta w_{,y} + A_{33}\, u_{,y}\, \delta w_{,y}) + \\ & + w_{,y} (A_{21}\, u_{,x}\, \delta w_{,y} + A_{23}\, u_{,y}\, \delta w_{,y} + A_{31}\, u_{,x}\, \delta w_{,x} + A_{33}\, u_{,y}\, \delta w_{,x}))\, dx\, dy \end{aligned}$$

$$\begin{aligned} K^{NL}_{15} = \int_{\Omega} (& w_{,x} (A_{12}\, v_{,y}\, \delta w_{,x} + A_{13}\, v_{,x}\, \delta w_{,x} + A_{32}\, v_{,y}\, \delta w_{,y} + A_{33}\, v_{,x}\, \delta w_{,y}) + \\ & + w_{,y} (A_{22}\, v_{,y}\, \delta w_{,y} + A_{23}\, v_{,x}\, \delta w_{,y} + A_{32}\, v_{,y}\, \delta w_{,x} + A_{33}\, v_{,x}\, \delta w_{,x}))\, dx\, dy \end{aligned}$$

$$K_{21}^{NL} = \int_{\Omega} \left(\frac{1}{2} w_{,y} (B_{12} w_{,y} \delta\psi_{x,x} + B_{32} w_{,y} \delta\psi_{x,y} + B_{13} w_{,x} \delta\psi_{x,x} + B_{33} w_{,x} \delta\psi_{x,y}) + \right.$$
$$\left. + \frac{1}{2} w_{,x} (B_{13} w_{,y} \delta\psi_{x,x} + B_{33} w_{,y} \delta\psi_{x,y} + B_{11} w_{,x} \delta\psi_{x,x} + B_{31} w_{,x} \delta\psi_{x,y}) \right) dx\, dy$$

$$K_{31}^{NL} = \int_{\Omega} \left(\frac{1}{2} w_{,x} (B_{21} w_{,x} \delta\psi_{y,y} + B_{31} w_{,x} \delta\psi_{y,x} + B_{32} w_{,y} \delta w_{y,y} + B_{33} w_{,y} \delta\psi_{y,x}) + \right.$$
$$\left. + \frac{1}{2} w_{,y} (B_{22} w_{,y} \delta\psi_{y,y} + B_{32} w_{,y} \delta\psi_{y,x} + B_{23} w_{,x} \delta\psi_{y,y} + B_{33} w_{,x} \delta\psi_{y,x}) \right) dx\, dy$$

$$K_{41}^{NL} = \int_{\Omega} \left(\frac{1}{2} w_{,x} (A_{11} w_{,x} \delta u_{,x} + A_{13} w_{,y} \delta u_{,x} + A_{31} w_{,x} \delta u_{,y} + A_{33} w_{,y} \delta u_{,y}) + \right.$$
$$\left. + \frac{1}{2} w_{,y} (A_{12} w_{,y} \delta u_{,x} + A_{32} w_{,y} \delta u_{,y} + A_{31} w_{,x} \delta u_{,x} + A_{33} w_{,x} \delta u_{,y}) \right) dx\, dy$$

$$K_{51}^{NL} = \int_{\Omega} \left(\frac{1}{2} w_{,x} (A_{21} w_{,x} \delta v_{,y} + A_{31} w_{,x} \delta v_{,x} + A_{23} w_{,y} \delta v_{,y} + A_{33} w_{,y} \delta v_{,x}) + \right.$$
$$\left. + \frac{1}{2} w_{,y} (A_{22} w_{,y} \delta v_{,y} + A_{32} w_{,y} \delta v_{,x} + A_{32} w_{,x} \delta v_{,y} + A_{33} w_{,x} \delta v_{,x}) \right) dx\, dy$$

References

[1] Ashton J. E. and Whitney J. M., 1970. *Theory of laminated plates.* Technomic Publishing Co. Inc.

[2] Bruno D., Leonardi A. and Porco G. *Nonlinear analysis of thick sandwich plates.* In «The Second East Asia-Pacific Conference on Structural Engng. and Constr., Chiang Mai, Thailand, 11-13 Jan. 1989».

[3] Calcote Lee R., 1969. *The analysis of laminated composite structures.* Van Nostrand Reinhold Company.

[4] Chia C. Y., 1980. *Non linear analysis of plates.* McGraw Hill Inc.

[5] Mindlin R. D., 1951. *Influence of rotatory inertia and shear on flexural motions of isotropic, elastic plates.* Journal of Appl. Mech.: 31-38.

[6] Pagano N. J., 1967. *Analysis of the flexure test of bidirectional composites.* J. Comp. Mater., 1, n. 4: 336-343.

[7] Pagano N. J., 1969. *Exact solution for composite laminates in cylindrical bending.* J. Comp. Mater., 3: 398-411.

[8] Pagano N. J., 1970. *Exact solutions for rectangular bi-directional composites and sandwich plates.* J. Comp. Mater., 4: 20.

[9] Pagano N. J., 1970. *Influence of shear coupling in cylindrical bending of anisotropic laminates.* J. Comp. Mater., 4: 330-343

[10] Panda S. C. and Natarayan R., 1979. *Finite element analysis of laminated composite plates.* Int. J. for Num. Meth. in Engng., 14: 69-79.

[11] Reddy J. N., 1984. *An introduction to the finite element method.* McGraw Hill Inc.

[12] Reddy J. N., 1984. *Energy and variational methods in applied mechanics.* John Wiley & Sons Inc.

[13] Reddy J. N. and Chao W. C., 1981. *Non linear bending of thick rectangular, laminated composite plates.* Int. J. Non Linear Mech., 16, n. 3/4: 291-301.

[14] Reissner E. and Stavsky Y., 1961. *Bending and stretching of certain types of heterogeneous aelotropic elastic plates.* Journal of Appl. Mech., 28: 402-408.

[15] Renn Kan Y. and Marvin Ito Y., 1972. *Analysis of unbalanced angle-ply rectangular plates.* Int. J. Solids Structures, 8: 1283-1297.

[16] Vinson J. R. and Chou T. W., 1975. *Composite materials and their use in structures.* Applied Science Publishers LTD, London.

[17] Whitney J. M. and Leissa A. W., 1969. *Analysis of heterogeneous anisotropic plates.* Journal of Appl. Mech: 261-301.

[18] Whitney J. M. and Pagano N. J., 1970. *Shear deformation in heterogeneous anisotropic plates.* Journal of Appl. Mech.: 1031-1036.